Thermal chemistry of copper(I)-*N,N′*-di-*sec*-butylacetamidinate on Cu(110) single-crystal surfaces

Qiang Ma and Francisco Zaera[a)]
Department of Chemistry, University of California, Riverside, California 92521

Roy G. Gordon
Department of Chemistry and Chemical Biology, Harvard University, Cambridge, Massachusetts 02138

(Received 2 August 2011; accepted 13 October 2011; published 3 November 2011)

The surface chemistry of copper(I)-*N,N′*-di-*sec*-butylacetamidinate on Cu(110) single-crystal surfaces has been characterized under ultrahigh vacuum by temperature programmed desorption (TPD) and X-ray photoelectron spectroscopy. A series of thermal stepwise conversions were identified, starting with the partial dissociative adsorption of the copper acetamidinate dimers into a mixture of monomers and dimers on the surface. An early dissociation of a C–N bond leads to the production of *N*-*sec*-butylacetamidine, which is detected in TPD experiments in three temperature regimes, the last one centered around 480 K. Butene, and a small amount of butane, is also detected above approximately 500 K, and hydrogen production, an indication of dehydrogenation of surface fragments, is observed at 460, 550 and 670 K. In total, only about 10% of the initial copper(I)-*N,N′*-di-*sec*-butylacetamidinate adsorbed monolayer decomposes, and only about ~3% of carbon is left behind on the surface after heating to high temperatures. The implications of this surface chemistry to the design of chemical film growth processes using copper acetamidinates as precursors are discussed. © *2012 American Vacuum Society*. [DOI: 10.1116/1.3658381]

I. INTRODUCTION

The growth of thin solid films of metals, oxides, nitrides, and other materials is an essential step in the manufacturing of microelectronic devices and in other industrial applications. Given the increasing demand for the deposition of such films conformally on structures with complex topographies at the nanometer scale, chemical-based film deposition methods have gained much relevance in recent years.[1–4] One key requirement in the design of chemical vapor deposition (CVD) processes is the identification of an appropriate compounds for the delivery of the elements to be deposited. Ideally, such compounds must be stable and volatile. In order to avoid the deposition of contaminants in the growing films, they should also display reasonably clean surface chemistry. An understanding of that surface chemistry can help in the design and selection of appropriate precursors for CVD processes.[5]

A large number of metallo-organic compounds have been tested for CVD applications. In many instances, in particular when late transition metals are involved, those are based on multiply coordinated ligands. Because of their high stability, ligands that coordinate in either bidentate (such as β-diketonates) or π (such as cyclopentadienyls) modes are common choices.[6] A promising family of bidentate ligands are acetamidinates. Indeed, acetamidinates of a number of transition metals have been successfully tested in recent years for both CVD and atomic layer deposition (ALD), a variation of CVD where the surface deposition is split into two time-separated and complementary reactions.[7,8] Copper acetamidinates in particular have shown exciting promise for both ALD and CVD of copper interconnects.[9–13] They have been used to grow metallic copper films with minimal incorporation of contaminants, a result that suggests that the precursors follow simple surface chemistry leading to the clean removal of the ligands.

Recent surface-science studies; however, suggest a more nuanced picture.[14–16] On SiO_2, copper(I)-*N,N′*-di-*sec*-butylacetamidinate has been reported to initially adsorb via displacement of one of the ligands at a surface hydroxide site.[15] Subsequent exposure to molecular hydrogen was proposed to lead to the hydrogenation of most of the remaining *N,N′*-di-*sec*-butylacetamidinates, and readsorption of some of the released *N,N′*-di-*sec*-butylacetamidine vapor was suggested as the source of the carbon contamination seen during the initial cycles of growth on silica. On metal surfaces, on nickel and cobalt substrates in particular, our earlier work indicated that the surface chemistry of the same precursor is significantly more complex, involving a series of stepwise reactions leading to the formation of adsorbed 2-butene and *N*-*sec*-butylacetamidine at ~200 K, acetonitrile and a *sec*-butylamido surface species around 400 K, and more dehydrogenated surface moieties above 485 K.[16] A temperature window was identified between approximately 350 and 450 K for the deposition of the precursor on the nickel and cobalt surfaces: lower temperatures are insufficient for activation of the dissociative adsorption, and higher temperatures lead to continuous decomposition beyond Cu monolayer saturation.[14]

Regardless of the initial substrate on which the copper films are grown, once a complete layer of copper is deposited, all subsequent growth takes place on that freshly deposited copper surface. In order to understand better how the film growth continues on copper, here we report on the results from our study on the surface chemistry of copper(I)-*N,N′*-di-*sec*-butylacetamidinate on a Cu(110) single-crystal

a)Author to whom correspondence should be addressed; electronic mail: zaera@ucr.edu

surface. Our results point to a lesser activity on copper than on nickel or cobalt substrates, an observation that may account for the slowing down of the film growth rate seen after initial nucleation on some surfaces. The copper acetamidinate follows surface chemistry on copper that is simpler but somewhat analogous to that seen on nickel, with cleavage to a smaller *N*-*sec*-butylacetamidinate intermediate and ultimately production of gas-phase butene. The details of this chemistry, and the implications for CVD and ALD processes, are discussed below.

II. EXPERIMENT

The experiments were conducted in an ultrahigh vacuum (UHV) system turbo-pumped to a base pressure of 1×10^{-10} Torr and equipped with an UTI mass quadruple for temperature programmed desorption (TPD), a concentric hemispherical analyzer (VG 100AX) and an Al K_α/Mg K_α dual-anode X-ray source for X-ray photoelectron spectroscopy (XPS), and a Kratos rasterable rare-gas ion gun for sample cleaning.[17] The XPS data were taken by using the Al K_α X-ray source ($h\nu = 1486.6$ eV), with a total resolution of approximately 1.0 eV, and the raw data were analyzed using deconvolution software in order to identify the different components of the overall signals in the spectra of each element.[16]

A polished Cu(110) single crystal was used as the substrate, a disk approximately 10 mm in diameter and 1 mm in thickness, mounted on a vacuum manipulator via 0.5 mm Ta wires wedged into slots filed onto the sides of the crystal and fixed to the ends of copper vacuum feedthroughs. Cooling was accomplished by using a liquid-nitrogen reservoir in direct contact with the copper feedthroughs, and resistive heating was used to reach any desired temperature between 90 and 1200 K. A K-type thermocouple was wedged into a hole drilled into the edge of the crystal to monitor the temperature of the surface, and a homemade temperature controller was used to provide linear temperature ramps for the TPD experiments and to maintain the crystal to within ± 1 K of any specified temperature. The heating rate for the TPD measurements was set to 10 K/s. A UTI quadrupole mass spectrometer, shielded with a retractable copper shroud with a small frontal opening for preferential detection of gases desorbing from the polished face of the single crystal, was used for the TPD experiments. A personal computer driven by home-written software was used to follow the evolution of as many as 15 amus simultaneously in a single TPD run. In the cases where the desorbing species displayed overlapping mass spectra, the TPD data were deconvoluted by following a procedure described in detail in a previous publication.[18] The Cu(110) crystal was cleaned before each experiment by repeated cycles of Ar^+ ion sputtering and annealing at 1100 K until the surface was deemed clean by XPS.

The copper(I)-*N,N′*-di-*sec*-butylacetamidinate precursor was synthesized by sequential reactions of *N,N′*-di-*sec*-butylacetamidine with CH_3Li and CuCl; the free *N,N′*-di-*sec*-butylacetamidine was prepared by reaction of acetonitrile with *N*-*sec*-butylamine.[19] All gases were purchased from Liquid Carbonic (Research Purity, >99.995%), and used without further treatment. Dosing of the sample was done by backfilling of the chamber using leak valves; in the case of the copper(I)-*N,N′*-di-*sec*-butylacetamidinate precursor, the gas line was heated to approximately 330 K in order to minimize condensation. Gas doses are reported in Langmuirs ($1\ \text{L} = 1 \times 10^{-6}$ Torr·s), uncorrected for differences in ion gauge sensitivities. The pressure in the main UHV chamber was measured using a nude ion gauge.

III. RESULTS

The thermal chemistry of copper(I)-*N,N′*-di-*sec*-butylacetamidinate on the Cu(110) single-crystal surface was first characterized by TPD experiments. Figure 1 displays the traces obtained after a 10.0 L dose at 90 K. Shown are, from top to bottom, data for hydrogen, butene, butane, copper(I)-*N,N′*-di-*sec*-butylacetamidinate (the molecular precursor), and *N*-*sec*-butylacetamidine. The signals for 2, 56, 58, 170, and 114 amu were chosen to report the evolution of those products in Fig. 1, respectively, but other masses were recorded as well to help with the identification of the products. The traces shown were corrected to eliminate the interferences from *N*-*sec*-butylacetamidine to the signals for butene and butane and the interferences from the molecular copper precursor to the signal for *N*-*sec*-butylacetamidine. No other desorbing product was identified in these experiments. The evolution of the TPD traces of each gas-phase product as a function of initial dose is shown in Fig. 2.

Several temperature regimes can be identified in the thermal chemistry of copper(I)-*N,N′*-di-*sec*-butylacetamidinate

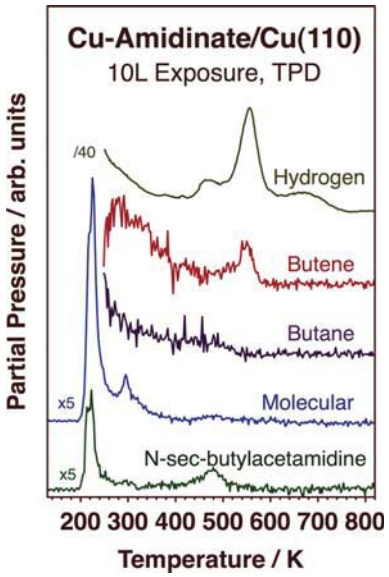

FIG. 1. (Color online) Survey TPD data from 10.0 L of copper(I)-*N,N′*-di-*sec*-butylacetamidinate dosed on Cu(110) at 90 K. Traces are shown for the desorption of the main products detected in the gas phase, namely (from top to bottom): hydrogen, butene, butane, the original copper(I)-*N,N′*-di-*sec*-butylacetamidinate, and *N*-*sec*-butylacetamidine. The signals for 2, 56, 58, 170 and 114 amu were used to follow these products, respectively.

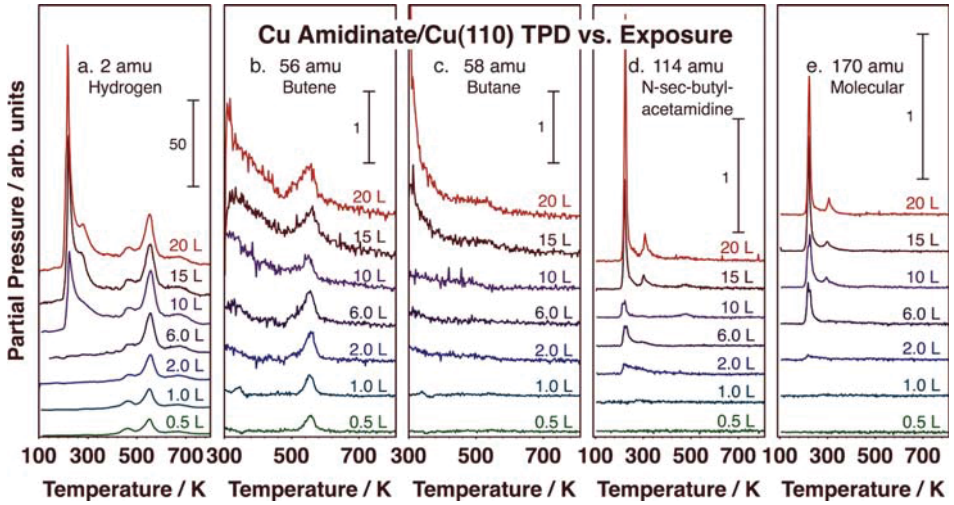

FIG. 2. (Color online) TPD traces for the main products from thermal activation of copper(I)-*N,N′*-di-*sec*-butylacetamidinate on Cu(110) as a function of initial dose at 90 K. From left to right, five panels are shown containing the data for hydrogen [Fig. 2(a)], butene [Fig. 2(b)], butane [Fig. 2(c)], *N*-*sec*-butylacetamidine [Fig. 2(d)], and the original copper(I)-*N,N′*-di-*sec*-butylacetamidinate [Fig. 2(e)].

on Cu(110) based on these TPD results. First, molecular desorption can be seen at temperatures below 300 K. A small feature is detected at 280 K after a 1.0 L dose, and a more intense peak, with a sharp leading edge and long high-temperature tail, starts to develop around 225 K by 2.0 L. These peaks, which correspond to desorption from the first monolayer, saturate after exposures of approximately 3 L, after which additional desorption from multilayer condensation is observed about 220 K. A third molecular desorption peak appears after doses of 10 L and above, initially at 295 K but at higher temperatures with increasing exposures, at 300 and 306 K for 15 and 20 L, respectively. The shift in temperature with changing surface coverage suggests nonlinear kinetics, possibly a reflection of the molecular species at this temperature being the result of a surface reaction. We propose that the copper(I)-*N,N′*-di-*sec*-butylacetamidinate that desorbs at ~300 K may be the result of recombination of monomers into dimers (the form in which the compound is believed to exist in the solid phase) on the surface (more on this later).[8] In principle, some of the peaks observed in the TPD traces for 170 amu could originate from *N,N′*-di-*sec*-butylacetamidine, from hydrogenation of the *N,N′*-di-*sec*-butylacetamidinate ligand. However, in all experiments, the signals for 170 and 171 amu parallel each other (after proper scaling), providing no indication for any additional desorbing products.

The production of a smaller acetamidine, *N*-*sec*-butylacetamidine, is also clearly observed in the TPD data. The two compounds are distinguished by their different cracking patterns in the mass spectrometer, as discussed in more detail in our previous publication.[16] Peaks are seen for 114 amu even at low temperatures, around 220 K, after high copper acetamidinate doses. It would appear that some degree of decomposition may take place on the original adsorbed precursor, simultaneously with molecular desorption. It could be thought that these signals may originate from cracking of the molecular species in the mass spectrometer, especially because the sharp nature of the peaks seen here makes their separation difficult. However, although that possibility cannot be completely ruled out, we do not think that this is the case: the relative shapes and intensity ratios of the peaks for 144 versus 170 amu vary considerably with dose, pointing to their origin from different species. In particular, significant *N*-*sec*-butylacetamidine is observed around 220 K (with a long high-temperature tail) after exposures as low as 2.0 L, at which point molecular desorption is almost negligible. Also, at higher coverages (6.0 and 10 L) the sharp low-temperature peaks that develop are split in the traces for both masses, but show different relative intensities and peak maxima for 114 versus 170 amu. Even the third peak, around 300 K, which is also seen for 114 amu, displays different behavior than that for 170 amu. We are reasonably confident that some *N*-*sec*-butylacetamidine is being produced both in the 215–225 K temperature range and also around 300 K. In addition, a small amount of *N*-*sec*-butylacetamidine desorbs at 480 K. The yields at this temperature are small, and seen in the 144 amu traces only at doses of 10 L or above. However, evidence for desorption of this species at lower coverages, after exposures as low as 0.5 L, was seen in the traces for 56, 57 and 58 amu (<10% of the signal after 10 L, data not shown).

The evolution of *N*-*sec*-butylacetamidine at 480 K is accompanied by desorption of small amounts of butane and butene, and also some hydrogen. The hydrogen desorbs at slightly lower temperatures, at about 460 to 470 K (depending on the initial coverage), indicating that the formation of the small acetamidine, which requires the addition of a hydrogen atom to the ligands in the initial copper precursor, is accompanied by other dehydrogenation surface reactions, possibly on the complementary *sec*-butyl moiety. The small amount of butane, another hydrogenation product (in this case, from *sec*-butyl moieties), is detected in a broad feature around 500–520 K, and is roughly matched by desorption of a similar amount (perhaps a bit more) of butene. It should be

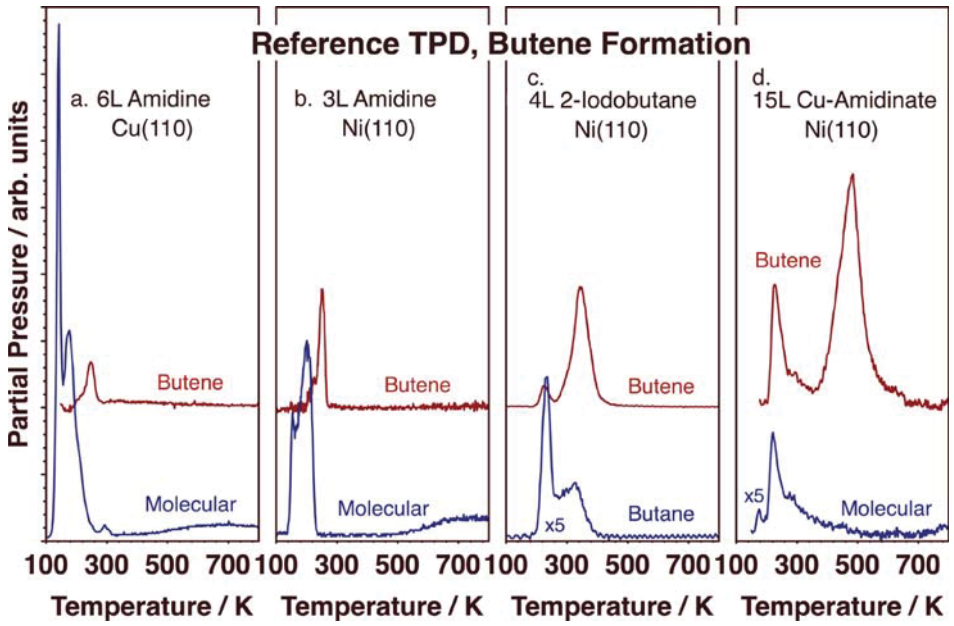

FIG. 3. (Color online) Reference TPD data, provided to aid in the interpretation of the thermal decomposition of copper(I)-*N,N′*-di-*sec*-butylacetamidinate on Cu(110) and Ni(110) surfaces. Shown are molecular (bottom traces) and butene (top traces) desorption traces for 6.0 L of *N,N′*-di-*sec*-butylacetamidine on Cu(110) [Fig. 3(a)], 3.0 L of *N,N′*-di-*sec*-butylacetamidine on Ni(110) [Fig. 3(b)], 4.0 L of 2-iodobutane on Ni(110) [Fig. 3(c)], and 15.0 L of copper(I)-*N,N′*-di-*sec*-butylacetamidinate on Ni(110) [Fig. 3(d)]. The data indicate that the high-temperature butene peak seen in the TPD of *N,N′*-di-*sec*-butylacetamidine on Cu(110) and Ni(110) surfaces does not originate from direct decomposition of adsorbed acetamidine or *sec*-butyl surface groups, and must involve a different intermediate, possibly a butylamido moiety.

noted that the yields of the reactions that take place in this ~450–520 K temperature regime are relatively small.

Much more significant amounts of butene and hydrogen desorb simultaneously around approximately 550 K. This reaction is observed even at very low coverages, and saturates rapidly, possibly because it occurs on surface species produced during the early stages of the uptake of the copper(I)-*N,N′*-di-*sec*-butylacetamidinate. The butene is most likely produced via β-hydride elimination from *sec*-butyl surface species, a common reaction on metal surfaces.[20,21] However, that *sec*-butyl moiety cannot exist as a stand alone species and is most likely still bonded to a nitrogen atom instead, possibly in an amido surface intermediate. Evidence for this conclusion is provided in Fig. 3, which shows TPD traces for selected reference systems. Specifically, data are provided for molecular and butene desorption from *N,N′*-di-*sec*-butylacetamidine adsorbed on Cu(110) and Ni(110) single-crystal surfaces (Figs. 3(a) and 3(b), respectively), and from 2-iodobutane and copper(I)-*N,N′*-di-*sec*-butylacetamidinate adsorbed on Ni(110) (Figs. 3(c) and 3(d), respectively). The data in the latter panel indicate similar high-temperature (485 K) butene formation on Ni(110),[16] and Figs. 3(a) and 3(b) show that the reaction is not likely to occur directly on the *N,N′*-di-*sec*-butylacetamidinate ligand, since that would decompose and produce butene at much lower temperatures, at about 250 K. Experiments with 2-iodobutane were carried out to determine the temperature range where β-hydride elimination occurs on *sec*-butyl intermediates bonded directly to the surface, by taking advantage of the fact that iodoalkanes can be used to produce alkyl surface species.[22,23] Figure 3(c) indicates that butene from *sec*-butyl surface species is produced at 320 K, a temperature in line with that reported for similar systems,[24–26] and much lower than what is seen here with the copper acetamidinate. It should be said that experiments with 2-butylamine on Ni(110) only showed molecular desorption, without formation of butene, but that may be because it is difficult to activate the amine to form surface amido groups. In any case, some amine could be retained on the surface to temperatures of up to 430 K (data not shown).

Further dehydrogenation of the surface species that remain after activation of copper(I)-*N,N′*-di-*sec*-butylacetamidinate adsorbed on Cu(110) at temperatures above 550 K, beyond butene formation, is manifested by the hydrogen desorption peak seen in Figs. 1 and 2 around 670 K. This hydrogen is likely to originate, at least in part, from further dehydrogenation of the butene that may remain on the surface.[27,28] It amounts to less than 20% of the total hydrogen detected; in contrast with the 60–70% associated with the 550 K peak. Assuming that all the H_2 at 550 K comes from β-hydride elimination of *sec*-butyl moieties, and that the H_2 in the 670 K feature comes from any remaining butyl and acetyl species left on the surface, the relative peak areas in the hydrogen TPD traces suggest that only about ~3% of the total carbon would be left behind on the surface by the final dehydrogenation steps. This is only a rough estimate, though, since it does not include the hydrogen consumed to make the hydrogenated products (*N-sec*-butylacetamidine, butane) or the change in overall stoichiometry due to desorption of fragments of the original ligand (*N-sec*-butylacetamidine, butene).

Additional information about the thermal chemistry of copper(I)-*N,N′*-di-*sec*-butylacetamidinate on Cu(110) was

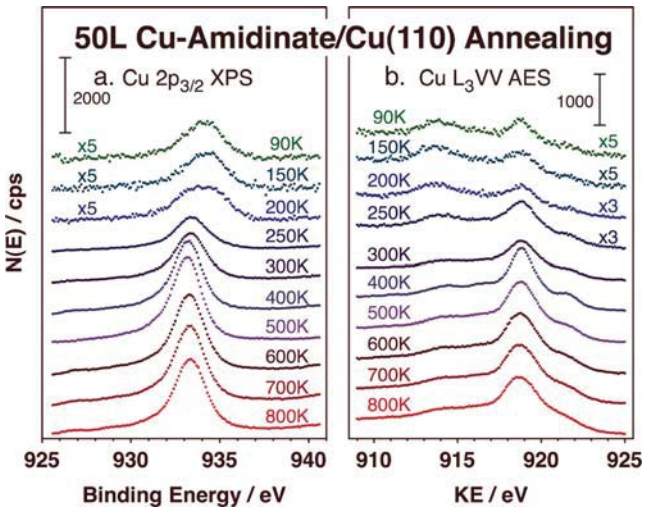

FIG. 4. (Color online) Cu $2p_{3/2}$ XPS [Fig. 4(a)] and Cu L_3VV Auger [Fig. 4(b)] data for a Cu(110) single-crystal surface dosed with 50 L of copper(I)-*N,N′*-di-*sec*-butylacetamidinate at 90 K as a function of subsequent annealing temperature. The signals from a condensed multilayer give way to those from the substrate upon molecular desorption between 200 and 250 K.

obtained by XPS. Figure 4 displays the data obtained for copper, for both the Cu $2p_{3/2}$ XPS [Fig. 4(a)] and the Cu L_3VV Auger [Fig. 4(b)] peaks, after dosing 50 L of the precursor on the Cu(110) surface at 90 K and annealing to the indicated temperatures, and Fig. 5 provides a summary of the peak areas [Fig. 5(a)] and peak positions [Fig. 5(b)] extracted from those data. Given that the substrate is a copper surface, it is not possible to follow the nature of the copper atoms deposited in the monolayer via decomposition of the copper acetamidinate (their signals are masked by the signal from the solid). However, the presence of a condensed multilayer at low temperatures is easily identified by the Cu $2p_{3/2}$ peak at 934.3 eV (binding energy) and the Cu L_3VV AES broad feature at around 913.7 eV (kinetic energy), and a transition is also clearly seen starting about 200 K, mostly by the broadening of the Cu $2p_{3/2}$ signal. That transition is nearly complete by 250 K, at which point new values are associated with the copper signals, at 933.3 and 918.8 eV, respectively, originating from the metallic copper substrate. The total signal intensities increase significantly during that transition, as the molecular copper acetamidinate from the condensed multilayer desorbs and the shielding provided by its organic ligands is reduced. Interestingly, the copper XPS and AES signals continue to grow with increasing annealing temperatures, all the way to approximately 500 K, indicating further stepwise removal of organic matter from the surface. This is consistent with the surface thermal chemistry identified by the TPD experiments. No evidence for the transitory formation of copper species in oxidation states other than the Cu(I) of the precursor or the Cu(0) of the metal surface was ever obtained.

The N 1s [Fig. 6(a)] and C 1s [Fig. 6(b)] XPS spectra corresponding to the same annealing sequence as that reported above for copper are provided in Fig. 6, and a summary of the peak areas in Fig. 7. In the latter, the evolution of the intensities versus annealing temperatures is provided for each of the key components identified via deconvolution of the data using Gaussian peaks. In the case of the carbon signal [Figs. 6(b) and 8(b)], the low-temperature spectra were deconvoluted by using three peaks, at 285.8, 286.15, and 287.6 eV, with the fixed 7:2:1 relative intensities expected from the alkyl, amido, and acetamidine carbon atoms in the molecular species, respectively [Fig. 8(b), bottom trace].[16] The overall calculated trace obtained by performing such fitting to the spectrum for 150 K was subtracted, after appropriate scaling, from the data recorded after annealing to higher temperatures. The sharp decrease seen in the intensity of that feature above 200 K reflects the desorption of molecular copper acetamidinate from the condensed multilayer, and

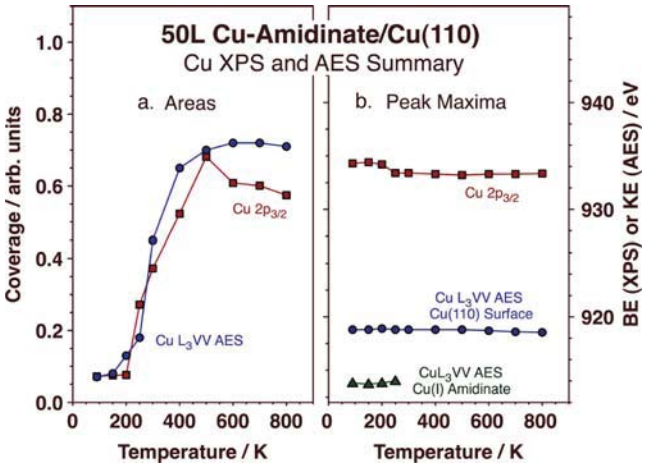

FIG. 5. (Color online) Summary of the copper XPS and AES data obtained for 50 L of copper(I)-*N,N′*-di-*sec*-butylacetamidinate dosed on Cu(110) at 90 K as a function of subsequent annealing temperature. The evolution of the peak areas [Fig. 5(a)] and peak position [Fig. 5(b)] are reported as a function of annealing temperature, indicating the unveiling of the substrate starting around 250 K.

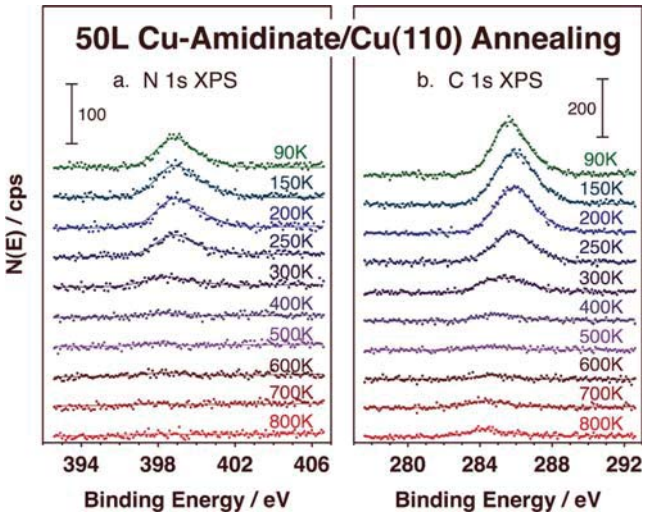

FIG. 6. (Color online) N 1s [Fig. 6(a)] and C 1s [Fig. 6(b)] XPS data from 50 L of copper(I)-*N,N′*-di-*sec*-butylacetamidinate dosed on Cu(110) at 90 K as a function of subsequent annealing temperature. The raw data are reported as dots, whereas the solid lines correspond to fits to multiple Gaussian peaks, as discussed in the text.

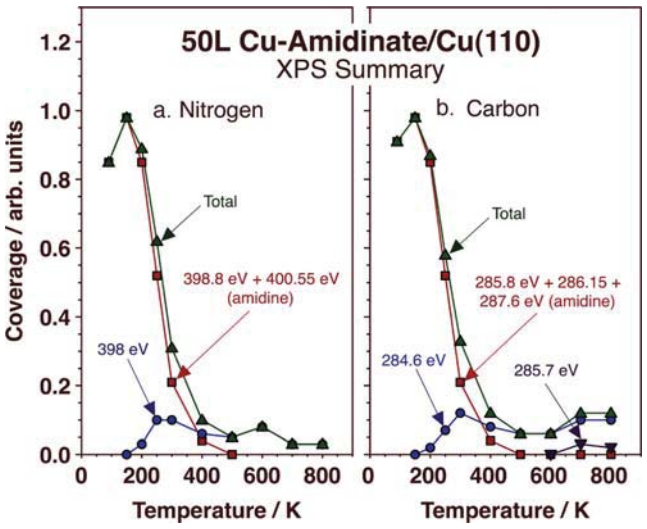

FIG. 7. (Color online) Summary of N 1s and C 1s XPS data for 50 L of copper(I)-*N,N′*-di-*sec*-butylacetamidinate dosed on Cu(110) at 90 K as a function of subsequent annealing temperature. Estimated surface coverages are reported for the different nitrogen [Fig. 7(a)] and carbon [Fig. 7(b)] peaks deconvoluted from the raw data in Fig. 6.

follows the similar changes observed in the copper XPS and AES data and the molecular desorption seen in the TPD experiments. A decreasing but measurable signal is nevertheless detected after annealing to temperatures up to 400 K, which we interpret as reflecting the presence of acetamidinate ligands adsorbed on the surface. About 50% of the original peak remains after annealing to 250 K [Fig. 8(b), top trace], a temperature above that required for molecular desorption according to the TPD data (Fig. 1), 20% after annealing to 300 K, following the desorption of both the molecular copper(I)-*N,N′*-di-*sec*-butylacetamidinate and *N*-*sec*-butylacetamidine from the first monolayer, and about 5% at 400 K, right before the surface chemistry that produces additional *N*-sec-butylacetamidine, butane, and butene gas products.

A similar molecular desorption and decomposition sequence as a function of annealing temperature is manifested by the N 1s XPS data. In this case, a broad feature was recorded for all low-temperature cases, composed of two peaks at 398.8 and 400.55 eV. This split is significant in that it indicates the presence of two chemically nonequivalent nitrogen atoms on the surface, as previously observed with copper(I)-*N,N′*-di-*sec*-butylacetamidinate adsorbed on Ni(110).[16] Given that the same split is seen with *N,N′*-di-*sec*-butylacetamidine but not with condensed copper(I)-*N,N′*-di-*sec*-butylacetamidinate multilayers, we have interpreted this observation as indicative of the dissociation of the dimer structure in which the precursor is believed to exist in the solid and gas phases upon adsorption.[19] The first feature, at 398.8 eV, has been assigned to the nitrogen atom coordinated to the copper ion in the original precursor, whereas the second peak at 400.55 eV reflects the existence of uncoordinated acetamidine nitrogen atoms. The one twist to this interpretation here is that while the relative intensities of the two N 1s XPS features from copper(I)-*N,N′*-di-*sec*-butylacetamidinate adsorbed on Ni(110)[16] and from *N,N′*-di-*sec*-butylacetamidine adsorbed on either Ni(110)[16] or Cu(110) [Fig. 9(a)] display similar intensities, the 398.8 eV:400.55 eV intensity ratio in the case of copper(I)-*N,N′*-di-*sec*-butylacetamidinate on Cu(110) is approximately 3:1. It would appear that, on Cu(110), only approximately half of the original copper acetamidinate dissociate into monomers in the first monolayer. It is also interesting to note that it is the latter 400.55 eV feature that becomes reduced preferentially upon annealing of the surface. This trend may be due to preferential conversion (or molecular desorption) of the species with uncoordinated nitrogens, but also points to a chemical transition leading to the formation of amido surface intermediates, as indicated by the new peak that remains around

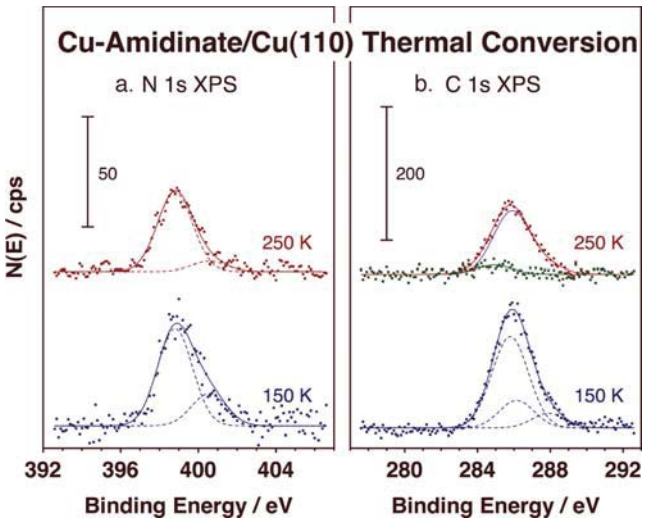

FIG. 8. (Color online) N 1s [Fig. 8(a)] and C 1s [Fig. 8(b)] XPS data from 50 L of copper(I)-*N,N′*-di-*sec*-butylacetamidinate dosed on Cu(110) at 90 K after annealing at 150 (bottom traces) and 250 (top traces) K. Also shown are the Gaussian peaks fitted to the data to highlight the main changes that take place on the adsorbed copper acetamidinate after molecular desorption.

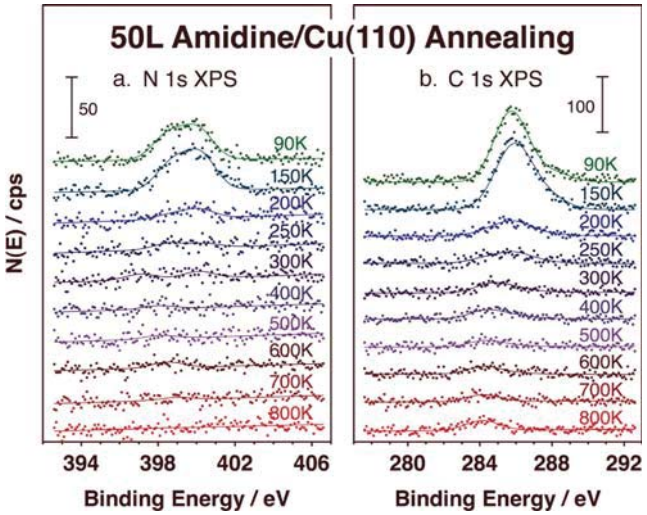

FIG. 9. (Color online) N 1s [Fig. 9(a)] and C 1s [Fig. 9(b)] XPS data from 50 L of *N,N′*-di-*sec*-butylacetamidine dosed on Cu(110) at 90 K as a function of subsequent annealing temperature. The raw data are reported as dots, Gaussian fits as solid lines.

398.0 eV at high temperatures. The N 1s XPS signal for molecular acetamidinate follows the very same trend versus annealing temperature seen in the C 1s XPS traces, and only about 5% of the total initial nitrogen remains on the surface above 500 K, in the form of amido moieties.

As indicated above, decomposition of some of the original acetamidinate on the surface, starting at temperatures as low as 200 K, is evidenced by the C 1s and N 1s XPS data, by the signal leftover after subtraction of the acetamidinate peaks from the spectra. The highlights of the XPS evidence for that transition are illustrated in Fig. 8, where the raw N 1s [Fig. 8(a)] and C 1s [Fig. 8(b)] XPS data are shown together with the appropriate fitted traces for the cases of 150 (bottom traces) and 250 (top traces) K annealing temperatures. The 150 K data are displayed with the Gaussian fits discussed above, namely, the 3:1 398.8 eV:400.55 eV double feature for the N 1s signal, and the 7:2:1 285.8 eV:286.15 eV:287.6 eV set of peaks associated with the C 1s trace. For the 250 K traces, those were deconvoluted into two components. In the case of the C 1s XPS, the overall molecular fit trace from the 150 K data was scaled appropriately (by a factor of 0.53 in this case) and subtracted from the raw data, and the residual data then fitted to a new Gaussian peak (centered at 284.9 eV in this case). The latter feature, which amounts to less than 10|% of the total C 1s XPS signal (7% in this case), reflects the formation of new aliphatic hydrocarbon surface species; its position does shift toward higher binding energies with increasing annealing temperature, until reaching a value of 285.7 eV at 500 K, indicating additional ongoing chemistry (dehydrogenation) at the surface. Yet another small C 1s XPS peak also develops around 285.6 eV above 600 K. That feature amounts to only 2–3% of the total initial carbon, and most likely corresponds to methylidyne or other highly dehydrogenated carbonaceous surface species deposited by decomposition of the acetamidinate ligand. It should be indicated that the high-temperature carbon seen at this point is not carbidic in nature, as those species display significantly lower C 1s XPS binding energies.[29]

Fitting of the N 1s XPS peaks was performed in two different ways, both of which yielded approximately the same information. In one, the scaled molecular peaks from the 150 K data were subtracted from the traces obtained for higher annealing temperatures, and the residual data then fitted to additional Gaussian peaks. The scaling factors used in this case were taken from the analysis of the C 1s XPS traces. This is the procedure followed to obtain the data reported in Fig. 7(a). Alternatively, the intensities of the two peaks seen for the molecular species, at 398.8 and 400.55 eV, were let to vary independently (the peak positions and widths were fixed in order to minimize the number of adjustable parameters). The results from the use of latter approach in the 250 K case, shown in Fig. 8(a), are particular useful to highlight the preferential decrease of the signal from the uncoordinated nitrogen atoms, the ones associated with the 400.55 eV peak. Indeed, in the data for the 250 K annealing temperature illustrated here, the original intensities for the 398.8 and 400.55 eV peaks seen at 150 K are reduced by 20 and 70%, respectively. This difference is seen in Fig. 7(a) by the extra intensity for amido nitrogen atoms indicated by the signal at 398 eV.

Finally, N 1s [Fig. 9(a)] and C 1s [Fig. 9(b)] XPS data are reported in Fig. 9 from reference experiments with 50 L of *N,N′*-di-*sec*-butylacetamidine dosed on Cu(110) at 90 K after annealing to the indicated temperatures. The signals for 90 and 150 K correspond to multilayers and a monolayer of the molecular acetamidine, respectively, as indicated by the desorption temperatures seen in TPD experiments [Fig. 3(a)]. Gaussian peaks were fitted to those traces following the same procedure used for the analysis of the copper(I)-*N,N′*-di-*sec*-butylacetamidinate data. For the C 1s XPS data, three Gaussian peaks were adjusted at 285.7, 286.6, and 288.2 eV, with fixed 7:2:1 area ratios. Notice that the binding energies of the amido and acetamidine carbons are somewhat different from those obtained for the copper acetamidinate precursor, indicating the lack of coordination to the Cu(I) ion. In the case of the N 1s XPS signals (for the 90 and 150 K traces), two peaks were fitted at 398.6 and 400.1 eV. The relative areas were freely adjusted but came out to be close to the expected 1:1 ratio; the low binding energy of the second nitrogen atom in this case may reflect the presence of an additional hydrogen atom.

Heating the adsorbed *N,N′*-di-*sec*-butylacetamidine to temperatures of 200 K and above induces extensive molecular desorption, but also leaves small amounts of carbon and nitrogen behind on the surface. In fact, the remaining C 1s XPS signal adds up to close to 10% of the initial intensity. That peak shifts gradually with increasing temperature, from about 284.6 eV at 300 K to 284.15 eV at 800 K, reflecting the stepwise dehydrogenation of the surface hydrocarbon intermediates. The N 1s XPS signal seen above 250 K is smaller in relative terms, about 5% or less, and centered at low binding energies, around 398 eV. The temperature trends seen for the acetamidine in these XPS data roughly follow those reported in Fig. 6 for the copper acetamidinate precursor.

IV. DISCUSSION

The TPD and XPS results reported here provide some insights into the thermal chemistry of copper(I)-*N,N′*-di-*sec*-butylacetamidinate adsorbed on Cu(110) single-crystal surfaces. The first general conclusion that can be reached is that such chemistry is stepwise and complex, taking place over a wide range of temperatures. A number of gas-phase products were detected in addition to the molecular copper precursor, mainly *N*-*sec*-butylacetamidine, butane, butene, and hydrogen, and a few additional surface intermediates can be proposed based on the XPS and TPD data, including adsorbed butene, copper(I)-*N*-*sec*-butylacetamidinate, acetonitrile, and a *sec*-butylamido surface moiety. Surface reactions could be identified up to temperatures as high as 700 K. The proposed reaction mechanism is shown schematically in Fig. 10.

This reaction mechanism of copper(I)-*N,N′*-di-*sec*-butylacetamidinate on Cu(110) is in many ways similar to what we have reported before on nickel and cobalt surfaces,[16] as it qualitatively involves the same reaction steps, intermediates,

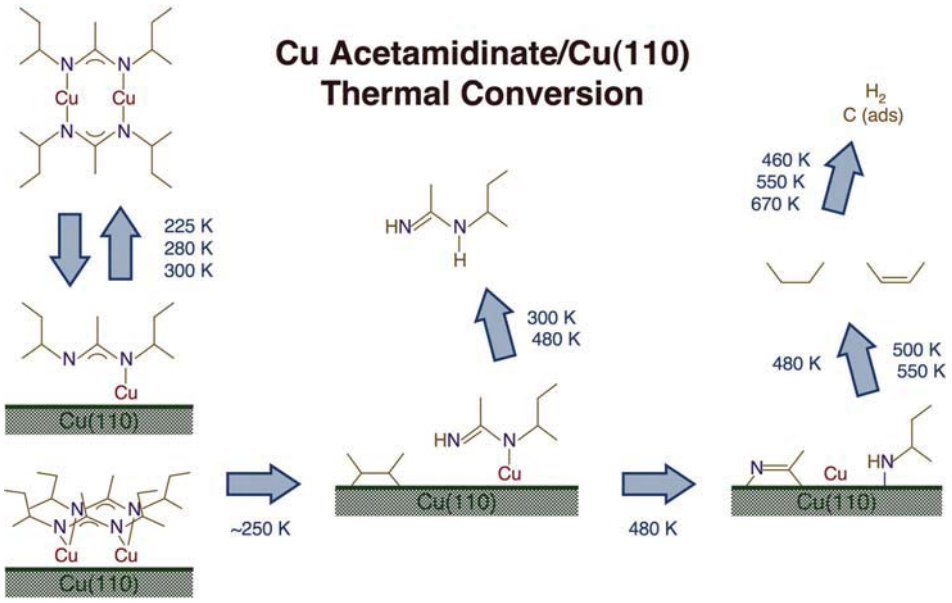

FIG. 10. (Color online) Schematic depiction of the main reactions proposed for the thermal chemistry of copper(I)-*N,N′*-di-*sec*-butylacetamidinate on Cu(110) single-crystal surfaces.

and products. Nevertheless, there are some important differences. For instance, while adsorption of copper(I)-*N,N′*-di-*sec*-butylacetamidinate on Ni(110) leads to the full dissociation of the dimer, on Cu(110) only approximately half of the adsorbed molecules split on the surface. It is also quite likely that this dissociation is partially reversible: we believe that the molecular desorption seen around 300 K in the TPD experiments may reflect that fact.

The reactivity of the copper acetamidinate precursor on copper also appears to be heavily dependent on its surface coverage. In particular, the data in Fig. 2 indicate that the reactions that produce most of the hydrogen and butene start at low coverages and saturate soon thereafter, whereas butane and *N*-*sec*-butylacetamidine production are only visible after high doses of the precursor. Moreover, the peak maxima of the TPD features for both copper(I)-*N,N′*-di-*sec*-butylacetamidinate and *N*-*sec*-butylacetamidine around 300 K shift significantly toward higher temperatures with increasing coverage. Lastly, most of the products display multiple peaks in the TPD, an observation that may be explained by the added stability of some surface intermediates at high coverages, when the surface is crowded and the decomposition pathways, which typically require empty sites, are blocked. As the temperature is increased and some adsorbates are removed from the surface via desorption of gas-phase products, surface sites open up, and additional conversion of the surface species may take place. This coverage dependence of the activity of the surface toward the decomposition of adsorbed copper(I)-*N,N′*-di-*sec*-butylacetamidinate needs to be taken into consideration when discussing chemical vapor deposition (CVD, ALD) processes, because under those circumstances the surface is continuously exposed to the copper acetamidinate at relatively high temperatures, so some decomposition takes place immediately upon adsorption. Consequently, higher reactivity is expected under CVD or ALD conditions than what is reported here based on TPD and XPS experiments, which start with low-temperature saturation.

The latter consideration takes particular meaning when realizing that the thermal conversion of copper(I)-*N,N′*-di-*sec*-butylacetamidinate on the Cu(110) surface seen here in TPD and XPS experiments is relatively low. Only about 10% of the initial monolayer goes on to decompose and form other products; according to the TPD data, approximately 90% desorbs molecularly. This reaction probability is significantly lower than those seen on nickel and cobalt substrates, where a third to half of the adsorbates react upon thermal activation.[14,16] The lesser reactivity of the copper surface is also indicated by the higher temperatures of reaction observed. For instance, the first C–N bond scission, responsible for the formation of the copper(I)-*N*-*sec*-butylacetamidinate intermediate, takes place by 200 K on nickel, but possibly at 250 K or higher temperatures on copper. It is particularly significant that some hydrogenation of that species to produce *N*-*sec*-butylacetamidine on Cu(110) occurs at 480 K; all the acetamidine detected from nickel desorbs at around 300 K. The same can be said of the butene emitted into the gas phase in these systems: the main TPD peak for that product is centered at 450 to 485 K on Ni(110) (depending on the initial coverage of the precursor), but only at approximately 550 K on Cu(110). Hydrogen desorption starts at 300 K on Ni(110), at 460 K on Cu(110).

A ~10% decomposition probability for copper(I)-*N,N′*-di-*sec*-butylacetamidinate on Cu(110) is certainly lower than those on other more active metal surfaces, but it is still reasonably high. Moreover, deposition rates under CVD or ALD conditions may be even higher than what this sticking coefficient may imply, for the reasons discussed above. In

fact, the copper acetamidinate precursor may be considered to be quite reactive on copper surfaces as far as film deposition applications is concerned. Perhaps more important, however, is the relative reaction probabilities seen for a given precursor on the different surfaces exposed during film growth. In relation with that, copper films deposited by CVD using this copper acetamidinate precursor are expected to grow at a slower rate on copper versus nickel or cobalt surfaces. Accordingly, in ALD processes, most of the deposition in the first half of the cycle would be expected on the nickel (or cobalt surfaces) all the way until those become fully covered, a preference that assures initial growth in two-dimensional fashion. Such behavior should lead to the build up of smooth films, although that also depends in part on the mechanism of growth after the deposition of the first layer, on the growing copper film.

In some instances, the deposition of copper films is carried out on nonmetal surfaces, for instance on the native oxide layer that forms on silicon wafers.[13,30,31] The reaction of copper acetamidinate precursors on such surfaces is believed to take place via a different mechanism, possibly starting on hydroxyl surface sites.[15] Oxide surfaces (SiO_2 and Al_2O_3) show a saturation density of chemisorbed copper acetamidinate three to four times larger than copper itself.[9] The present results indicate that copper acetamidinate chemisorbs dissociatively into several species on copper, each blocking one or more surface sites. In contrast, adsorption on hydroxylated surfaces, such as oxides, leads to the immediate release of at least one ligand as a free acetamidine containing hydrogen from a surface hydroxyl group, while the remaining surface-bound species remains intact after chemisorption. Thus, there is room to chemisorb a greater density of copper amidinate on oxides than on copper.

Finally, a brief discussion is provided on the purity of the films that may be deposited by using copper(I)-*N,N′*-di-*sec*-butylacetamidinate as the precursor in CVD or ALD processes. Ideally, the precursor used for metal deposition should contain stable ligands that remain intact upon adsorption and are easily removed by the second reactant, hydrogen in the case of acetamidinate metal complexes. In reality, we have shown that in most cases the surface chemistry involved is much more complex, generating a series of surface intermediates over a wide range of temperatures.[5,32–37] This is certainly true for the case of copper(I)-*N,N′*-di-*sec*-butylacetamidinate on nickel or cobalt surfaces, where an upper limit of approximately 450–480 K was identified for clean copper film deposition. Even though the acetamidinate ligands start decomposing at much lower temperatures, the first products of that chemistry are intermediates that may be easily hydrogenated. Specifically, the *N-sec*-butylacetamidinate produced via an initial C–N bond breaking can be hydrogenated to gas-phase *N-sec*-butylacetamidine, a reaction that occurs to some extent even in the absence of added hydrogen. The next set of products, butene in particular, can also potentially desorb from the surface intact. Only at high temperatures the surface intermediates that are produced are bonded irreversibly, and are expected to leave carbon and nitrogen impurities within the metal film. Fortunately, since the decomposition chemistry is slower on copper than on nickel or other more active transition metals, irreversible decomposition takes place at higher temperatures. Therefore a wider range of temperatures is available for copper CVD or ALD on the growing copper film. Recall in particular that some *N-sec*-butylacetamidine desorption was detected here at 480 K, indicating that even those high temperatures may be safe for clean film growth. Also, the surfaces annealed at higher temperatures in our study show only a few percent (~3%) of carbon contamination in the XPS data.

Based on the surface chemistry described here, it can be said that the use of copper acetamidinate precursors to grow copper films is quite promising, and may lead to the deposition of clean copper films as long as the surface intermediates can be hydrogenated effectively by the second reactant (H_2). Dissociation of H_2 on the copper surface and promotion of these hydrogenation reactions may be the limiting factor in these copper thin film chemical depositions. This is particularly true because molecular hydrogen adsorption on copper is activated, and the equilibrium between gas-phase H_2 and adsorbed H atoms almost energy neutral. In Fig. 11 we show the equilibrium isotherms calculated for hydrogen on Cu(110) based on reported kinetic parameters.[38–40] It can be seen there that detectable coverages of atomic hydrogen on the surface are only possible in the presence of H_2 gas at pressures above approximately 10^{-3} bar (~1 Torr), at which point the coverage is still less than 1% of monolayer saturation. Also, because of the near thermal neutrality of the reaction, similar steady-state surface coverages are obtained over a wide temperature range. This is in contrast to what is seen with most other transition metals, where the adsorption is nonactivated, and where higher coverages can be achieved at lower temperatures.[14] Ultimately, hydrogen treatments in CVD or ALD processes require the use of H_2 pressures of at

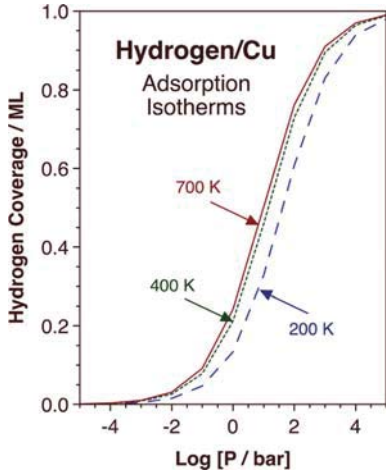

FIG. 11. (Color online) Estimated steady-state hydrogen surface coverages on Cu(110) as a function of hydrogen pressure and surface temperature, calculated using adsorption and desorption parameters from the literature.[38–40] Traces are shown for three temperatures, 200, 400 and 700 K, covering the temperature range of interest in ALD. At all temperatures, significant hydrogen coverages are only possible in the presence of relatively high H_2 pressures, above approximately 10^{-3} bar (~ 1 Torr).

least a few Torr to be effective. Also, any hydrogenation of the surface species left behind by decomposition of the metal precursor needs to occur during that exposure; no residual surface hydrogen is available after pumping to prepare the substrate for further adsorption in the next cycle in ALD processes.

V. CONCLUSIONS

The thermal chemistry of copper(I)-*N,N′*-di-*sec*-butylacetamidinate on Cu(110) surfaces follows the multistep mechanism schematically summarized in Fig. 10. Adsorption of the copper acetamidinate dimer from the gas phase leads to its partial dissociation and to the deposition of approximately 50% of dimers and 50% of monomers on the surface. Molecular desorption is seen in three stages, from condensed multilayers at about 225 K, from the first monolayer at around 280 K, and via monomer recombination in the 300 K range. These molecular desorption regimes are accompanied by production of some *N-sec*-butylacetamidine, presumably via a C–N bond scission followed by hydrogenation. Additional *N-sec*-butylacetamidine desorption is seen at 480 K, pointing to the stability of the originating surface *N-sec*-butylacetamidinate intermediate, and further surface reactivity is evidenced by desorption of a combination of a small amount of butane and butene, together with some hydrogen, at temperatures slightly below 500 K. Larger yields of butene and hydrogen are then detected at 550 K, the result of a β-hydride elimination step on another hydrocarbon surface intermediate, most likely a butylamido species. Finally, a H_2 desorption peak at 670 K reflects the final dehydrogenation steps of the irreversibly adsorbed hydrocarbon adsorbates produced by this chemistry, which leaves approximately 3% of carbon on the surface.

The complex surface chemistry of copper(I)-*N,N′*-di-*sec*-butylacetamidinate on copper surfaces identified here is of relevance to the deposition of copper thin films by chemical means using this precursor. The decomposition probability of the copper acetamidinate is approximately 10%, significantly lower than on other more active transition metal surfaces or on oxide surfaces such as silicon oxide. This relative low probability of copper deposition on itself can explain the change in deposition rate as the copper films grow in processes using the copper acetamidinate compound. On the other hand, the high temperatures needed for the decomposition of the first surface intermediates, *N-sec*-butylacetamidinate in particular, offers a wide temperature window for the chemical vapor deposition (CVD) or atomic vapor deposition (ALD) of copper films cleanly, without the incorporation of significant amounts of impurities. That; however, hinges on the effective hydrogenation of the surface fragments, which requires hydrogen pressures on the order of a few Torr or more.

ACKNOWLEDGMENTS

Funding for this project was provided by the U. S. Department of Energy, Materials Science Division, under Grant No. DE-FG02-03ER46599.

[1]M. Leskelä and M. Ritala, Angew. Chem., Int. Ed. **42**, 5548 (2003).
[2]J. E. Crowell, J. Vac. Sci. Technol. A **21**, S88 (2003).
[3]M. Schumacher, P. K. Baumann, and T. Seidel, Chem. Vap. Deposition **12**, 99 (2006).
[4]M. Ritala and J. Niinistö, ECS Trans. **25**, 641 (2009).
[5]F. Zaera, J. Mater. Chem. **18**, 3521 (2008).
[6]M. Putkonen and L. Niinistö, Top. Organomet. Chem. **9**, 125 (2005).
[7]B. S. Lim, A. Rahtu, and R. G. Gordon, Nature Mater. **2**, 749 (2003).
[8]B. S. Lim, A. Rahtu, J. S. Park, and R. G. Gordon, Inorg. Chem. **42**, 7951 (2003).
[9]Z. Li, A. Rahtu, and R. G. Gordon, J. Electrochem. Soc. **153**, C787 (2006).
[10]H. Kim, H. B. Bhandari, S. Xu, and R. G. Gordon, J. Electrochem. Soc. **155**, H496 (2008).
[11]S. O. Kucheyev, J. Biener, T. F. Baumann, Y. M. Wang, A. V. Hamza, Z. Li, D. K. Lee, and R. G. Gordon, Langmuir **24**, 943 (2008).
[12]V. Krisyuk, A. N. Gleizes, L. Aloui, A. Turgambaeva, B. Sarapata, N. Prud'Homme, F. Senocq, D. Samelor, A. Zielinska-Lipiec, D. de Caro, and C. Vahlas, J. Electrochem. Soc. **157**, D454 (2010).
[13]Y. Au, Y. Lin, and R. G. Gordon, J. Electrochem. Soc. **158**, D248 (2011).
[14]Q. Ma, H. Guo, R. G. Gordon, and F. Zaera, Chem. Mater. **22**, 352 (2010).
[15]M. Dai, J. Kwon, M. D. Halls, R. G. Gordon, and Y. J. Chabal, Langmuir **26**, 3911 (2010).
[16]Q. Ma, H. Guo, R. G. Gordon, and F. Zaera, Chem. Mater. **23**, 3325 (2011).
[17]D. Chrysostomou, J. Flowers, and F. Zaera, Surf. Sci. **439**, 34 (1999).
[18]J. Wilson, H. Guo, R. Morales, E. Podgornov, I. Lee, and F. Zaera, Phys. Chem. Chem. Phys. **9**, 3830 (2007).
[19]Z. Li, S. T. Barry, and R. G. Gordon, Inorg. Chem. **44**, 1728 (2005).
[20]F. Zaera, Chem. Rev. **95**, 2651 (1995).
[21]Z. Ma and F. Zaera, Surf. Sci. Rep. **61**, 229 (2006).
[22]F. Zaera, Acc. Chem. Res. **25**, 260 (1992).
[23]S. Tjandra and F. Zaera, J. Vac. Sci. Technol. A **10**, 404 (1992).
[24]J.-L. Lin and B. E. Bent, J. Am. Chem. Soc. **115**, 6943 (1993).
[25]S. Tjandra and F. Zaera, J. Am. Chem. Soc. **117**, 9749 (1995).
[26]S. Tjandra, H. Guo, and F. Zaera, Top. Catal. **54**, 26 (2011).
[27]I. Lee and F. Zaera, J. Phys. Chem. B **109**, 2745 (2005).
[28]I. Lee and F. Zaera, J. Phys. Chem. C **111**, 10062 (2007).
[29]*Handbook of X-Ray Photoelectron* Spectroscopy, edited by C. D. Wagner, W. M. Riggs, L. E. Davis, J. F. Moulder, and G. E. Muilenberg (Perkin-Elmer Corporation, Eden Prairie, 1978).
[30]J. Iijima, Y. Fujii, K. Neishi, and J. Koike, J. Vac. Sci. Technol. B **27**, 1963 (2009).
[31]T. Waechtler, N. Roth, R. Mothes, S. Schulze, S. E. Schulz, T. Gessner, H. Lang, and M. Hietschold, ECS Trans. **25**, 277 (2009).
[32]M. Xu, H. Tiznado, B.-C. Kang, M. Bouman, I. Lee, and F. Zaera, J. Korean Phys. Soc. **51**, 1063 (2007).
[33]H. Tiznado, M. Bouman, B.-C. Kang, I. Lee, and F. Zaera, J. Mol. Catal. A: Chem. **281**, 35 (2008).
[34]B.-C. Kan, J.-H. Boo, I. Lee, and F. Zaera, J. Phys. Chem. A **113**, 3946 (2009).
[35]M. Bouman and F. Zaera, ECS Trans. **33**, 291 (2010).
[36]T. Kim and F. Zaera, J. Phys. Chem. C **115**, 8240 (2011).
[37]M. Bouman and F. Zaera, J. Electrochem. Soc. **158**, D524 (2011).
[38]J. M. Campbell and C. T. Campbell, Surf. Sci. **259**, 1 (1991).
[39]M. Johansson, O. Lytken, and I. Chorkendorff, J. Chem. Phys. **128**, 034706/1 (2008).
[40]G. Anger, A. Winkler, and K. D. Rendulic, Surf. Sci. **220**, 1 (1989).